PHYSICAL REVIEW E, VOLUME 65, 035205(R)

Spatial forcing of spontaneous optical patterns

R. Neubecker and A. Zimmermann
Institute of Applied Physics, Darmstadt University of Technology, Hochschulstraβe 6, 64289 Darmstadt, Germany
(Received 30 August 2000; revised manuscript received 4 October 2001; published 27 February 2002)

A nonlinear optical system, which spontaneously forms hexagonal patterns, is exposed to a weak, spatially modulated forcing. As forcing, stationary hexagonal patterns are used under variation of their transverse wave number. In the experiment, we observe a locking when the forcing wave number is close to one of the critical wave numbers of the unforced system. Outside the locking regimes, forcing provokes spatiotemporal disorder. The system response is characterized quantitatively with respect to its dynamics and to its spatial order.

DOI: 10.1103/PhysRevE.65.035205 PACS number(s): 05.45.Jn, 42.65.Sf, 42.60.Jf, 47.54.+r

Many modern optical systems fulfill the prerequisites for the occurrence of spatial instabilities: they are spatially extended, nonlinear, and far from thermodynamic equilibrium. Today, spontaneous optical patterns are investigated in a variety of optical architectures and nonlinear materials [1]. On a macroscopic level, the emerging patterns resemble very much those well known from other disciplines, like fluid dynamics, chemical oscillations, or biology [2]. However, the physical mechanisms are completely dissimilar. One important peculiarity of optics is that transport of information is not associated with the transport of mass.

Optics opens new access to the investigation of the physics of pattern formation, in particular, through concepts which are hard to realize experimentally in other disciplines. One example is the minimal invasive control and stabilization of unstable patterns [3,4]. Another example is the topic of this Rapid Communication: spatial forcing [5].

As known from purely temporal systems, the response of nonlinear oscillators to external stimuli can be very complex [8]. In the case of extended systems, there is the additional degree of freedom in the spatial modulation of the forcing signal. Recent work often dealt with a time-dependent, but spatially uniform perturbation [9]. In the following, we will instead consider a static, but spatially modulated perturbation applied to a system which exhibits a stationary bifurcation to patterns.

Experimentally, spatial forcing is not simple to realize, e.g., in fluids or chemical oscillations, because one needs to manipulate system quantities in space and time. In optics, the possibility to superpose light waves makes it simple to introduce external, spatially modulated signals. This advantage can be utilized in other systems if the nonlinearity is made photosensitive [9].

A previous experiment covered spatial forcing of roll patterns in an electrofluid dynamical system [10]. In this quasi-one-dimensional case, a locking of the system state onto the forcing pattern was observed for certain commensurate ratios of spatial forcing and spontaneous wave number. The open question is what happens for fully two-dimensional patterns.

Spatial forcing of an optical system has previously been investigated in numerical simulations of a two-level medium in a cavity [6]. We instead use a single-feedback experiment containing a Kerr-type nonlinearity [11–13].

Forcing is realized by superposition of an additional light wave with a particular intensity profile. The forcing patterns are chosen to have the same hexagonal symmetry as the spontaneous ones, but with varying wave numbers. This drives the system into one of two distinct states: either it reproduces the forcing pattern (*locking*) or it responds with spatiotemporal disorder. To obtain a quantitative picture, we will reduce the complex spatiotemporal system response to single measures for the global dynamics and for the spatial order.

In the experiment, the Kerr-type nonlinearity is provided by a *liquid crystal light valve* (LCLV), which allows us to realize large aspect ratio patterns with laser powers of some ten milliwatts only. The LCLV is a multilayer device with an intensity sensitive photoconductor layer (write side) and a liquid crystal layer (read side). Both are separated by a dielectric mirror. To couple the layers, an electric field is applied by sandwiching transparent electrodes. In such a way, the refractive index of the liquid crystal layer changes with the light intensity at the write side. A light wave which is reflected by the LCLV read side acquires a phase profile which corresponds to the intensity profile at the write side.

The LCLV is put into an optical feedback loop (Fig. 1): a uniform laser beam (pump) is phase modulated and reflected by the LCLV read side. The modulated beam is guided back to the write side. In the feedback loop, higher spatial frequencies can be cut off by an optical low-pass filter. During the propagation through the feedback loop, diffraction transforms spatial phase modulations back into intensity modulations.

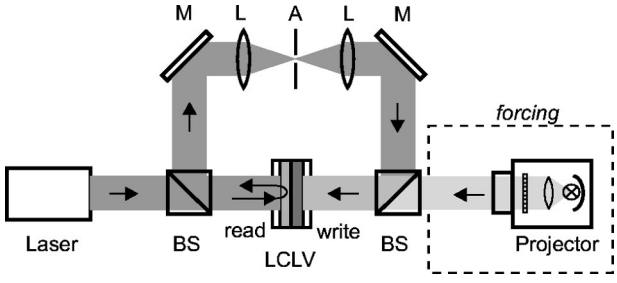

FIG. 1. Simplified scheme of the experimental setup. From the left, an expanded laser beam is incident onto the liquid crystal light valve (LCLV) read side. The phase modulated wave is reflected and guided to the write side by beam splitters (BS) and mirrors (M). Two lenses (L) and an aperture (A) form a spatial low pass filter. The forcing light wave is generated by a data projector and coupled into the system by a beam splitter. Not shown are the components for detection and imaging purposes.

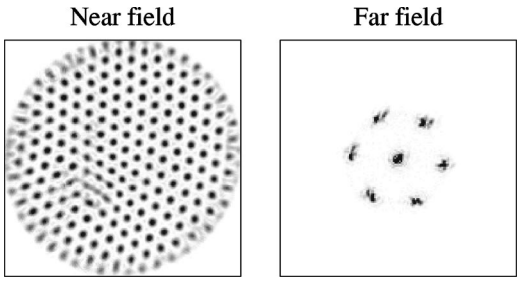

FIG. 2. Example of a spontaneous pattern (left-hand side) and the corresponding far field (right-hand side) in inverse gray scale: dark corresponds to high intensity. The active area has a diameter of 6 mm. The average of the forcing intensity shifts the operating point of the LCLV. Therefore, this image has been taken with a uniform forcing intensity corresponding to the average of the forcing patterns applied later.

Since the optical feedback is almost instantaneous, the system dynamics is determined by the relaxation-type response of the LCLV (in the order of tens of milliseconds). The system can be described by an equation for the phase shift $\Phi(x,y,t)$ induced by the LCLV (Eq. 1) and by one for the feedback wave intensity (Eq. 2) [13]

$$\tau\dot{\Phi} - l^2\nabla_\perp^2\Phi + \Phi = \Phi_{max}\left[1 - \tanh^2\left(\frac{1+\kappa_r(I_w+I_f)}{1+\kappa_s(I_w+I_f)}\hat{V}_{ext} - \hat{V}_{th}\right)\right], \quad (1)$$

$$I_w = |\exp[-i(L/2k_0)\nabla_\perp^2]\exp(-i\Phi)|^2 I_p . \quad (2)$$

Here, $\Phi_{max}, \kappa_r, \kappa_s, \hat{V}_{ext}, \hat{V}_{th}$, and l are LCLV parameters. Diffraction is covered by the operator $\exp[-i(L/2k_0)\nabla_\perp^2]$, with the propagation length L (here, $L=30$ cm) and the light wavelength λ (here, $\lambda=532$ nm). $\nabla_\perp^2$ is the Laplacian in the transverse coordinates x,y.

The laser pump intensity is I_p, and the feedback intensity at the LCLV write side is $I_w(x,y,t)$. This intensity distribution is recorded in the experiment and is also the quantity on which we act with the forcing intensity field $I_f(x,y)$. The optical far field, i.e., the spatial power spectrum of the feedback light field is recorded as well.

A linear stability analysis of the unforced system shows that above a certain pump intensity threshold, the uniform state becomes modulationally unstable with respect to a particular transverse wave number $k_c \approx \sqrt{3/(2\lambda L)}$ [11,13]. In the largest part of the parameter space, this leads to patterns of hexagonally arranged bright spots (Fig. 2). There are also higher-order critical wave numbers $k_c^{(n)} \approx \sqrt{[(4n-1)/3]}k_c$, but with higher thresholds. When increasing pump intensity further above threshold, spatial order breaks up and dynamics sets in [14,15].

Forcing is realized by coupling an additional, incoherent light wave into the given feedback loop. A standard data projector with a white light source serves to generate almost arbitrary forcing signals, focused onto the LCLV write side (Fig. 1). The projector intensity is attenuated to correspond to about 20% of the intensity of the feedback wave. There is an enormous degree of freedom in choosing the spatial (and temporal) structure of the forcing signal. As a first step, we use static hexagonal patterns, varying their wave number k_f.

The presence of higher wave numbers can have different effects on the pattern formation process. Harmonics have been proven to be necessary to stabilize particular patterns, like squares or quasipatterns [4,16]. However, we have never experimentally observed these ordered patterns in our free running system. Instead, the presence of higher critical wave numbers here only promotes the occurrence of spatiotemporal disorder [14,15].

We can now focus on the two basic wave numbers, namely, the critical one k_c and the one of the forcing pattern k_f by suppressing higher wave numbers with the spatial low-pass filter. When the forcing wave number is smaller than the spontaneous one $k_f \leqslant k_c$, the low-pass cutoff is set just above the critical wave number. For larger forcing wave numbers, however, this setting would cut off the forcing itself. Therefore, for $k_f > k_c$, the low pass was opened to $2k_c$ (due to diffusion, even larger wave numbers are barely excited anyway). This allows the excitation of harmonics and higher critical wave numbers.

The pump intensity is chosen well above threshold, where the spontaneous pattern already begins to loose spatial order (cf. Fig. 2). It consists of large ordered domains with moving boundaries and/or few localized defects. The system runs for a while, before forcing is switched on. After about 30 seconds, when the system appeared to have reached an asymptotic state, sequences of intensity patterns were recorded. The measurement was divided into two parts ($k_f > k_c$ and $k_f \leqslant k_c$). When approaching $k_f \approx k_c$ from large forcing wave numbers, the system appeared to drift, requiring a readjustment.

We observe two distinct types of system response: either the system locks onto the forcing and shows stationary and highly ordered patterns, which correspond exactly to the forcing pattern (the response pattern even follows a rotating forcing pattern up to a certain angular velocity). In the other case, the response is quite dynamic and spatially disordered (''turbulent''). Examples of snapshots are shown in Fig. 3.

From the corresponding far fields, also shown in Fig. 3, we can take that in almost all cases the optical power is mainly concentrated in (modes on) the annulus belonging to the first critical wave number k_c. The only exception is the locking regime close to $k_f/k_c \approx 1.6$, where the power is mainly in these higher modes.

In the locking regimes, the far-field modes are clearly hexagonal and very localized. Outside the locking regimes, and for small forcing wave numbers we find broadened hexagonal modes. As the forcing wave number further increases—still outside the locking regimes—the broadened modes gradually transform into an excitation of the full critical wave number annulus (cf. Fig. 3). In real space, this corresponds to an increasing number of local defects and boundaries between domains of decreasing size until the pattern is too disordered to describe it in terms of defects. For high forcing wave numbers, also domains of rolls appear in the system response.

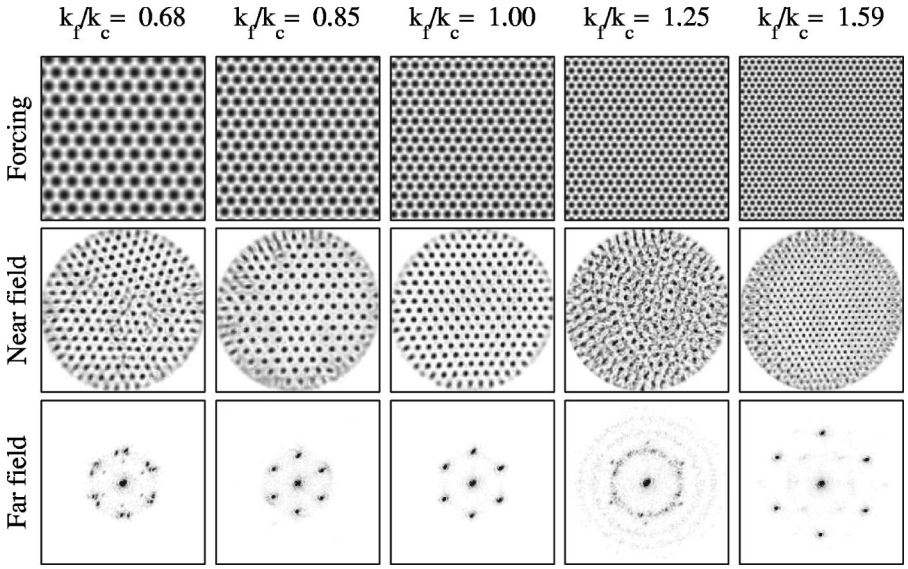

FIG. 3. Forcing and system response for different ratios k_f/k_c between forcing and spontaneous wave number. The upper row shows the synthesized forcing patterns, the middle row shows the corresponding system response, and the lower row presents the corresponding far fields.

We use two complementary approaches to derive quantitative measures from the system response. First, disregarding the spatial structure, the dynamics is characterized by a temporal autocorrelation, averaged in space

$$\langle K(\Delta t)\rangle_{x,y} = \int \hat{I}_w(x,y,t-\Delta t)\hat{I}_w(x,y,t)dt\,dx\,dy. \quad (3)$$

$\hat{I}_w(x,y,t) = I_w - \overline{I_w}$ is the recorded intensity sequence $I_w(x,y,t)$, subtracted by its average $\overline{I_w}$. From the autocorrelation functions, we can extract as characteristic quantity the time constant τ_s of the first steep decay (Fig. 4, inset). The dependence of τ_s on the forcing wave number is shown in Fig. 4.

As a second approach, we consider spatial order only by measuring the degree of hexagonal symmetry [17]. We again use autocorrelation functions, now correlating an individual snapshot to its rotated counterpart,

$$C(\theta,x_0,y_0) = \int \hat{I}_w(x,y)\hat{I}_w(x',y')dx\,dy, \quad (4)$$

x',y' being the rotated coordinates and θ the rotation angle. This is done for many rotation centers (x_0,y_0), over which we average $C(\theta,x_0,y_0) \rightarrow \langle C(\theta)\rangle$. Hexagonal order is reflected in peaks at every $\theta = n\times 60°$ (Fig. 5, inset). The amplitude of these peaks can be summarized in a single number H, the hexagonal symmetry parameter. The average of the symmetry parameters found for the images of each sequence is plotted in Fig. 5 over the forcing wave number. The three data points just above $k_f = k_c$ (not connected by the dashed line) are probably outliers, caused by the above-mentioned drift.

Both the temporal and the spatial measure display the same behavior. We identify a regime of strong spatial locking around $k_f \approx k_c$, where the response is stationary (diverging τ_s) and highly ordered (large value of H), matching the forc-

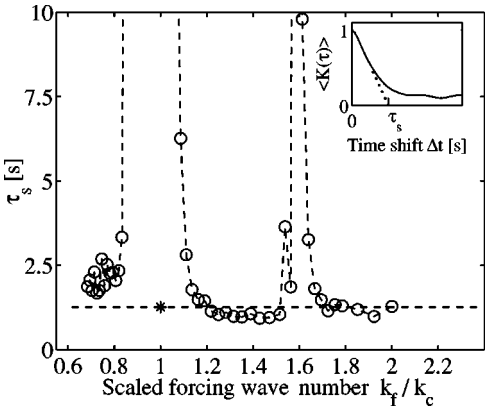

FIG. 4. Characterization of the response dynamics: plot of the short-term decay time constant τ_s of the temporal autocorrelation function versus the ratio k_f/k_c between forcing and critical wave number. The value for the unforced system (- - ∗ - -) is included for comparison. Two locking regimes of stationary system response exist where τ_s diverges. The inset shows a typical temporal autocorrelation function and the linear fit to determine τ_s.

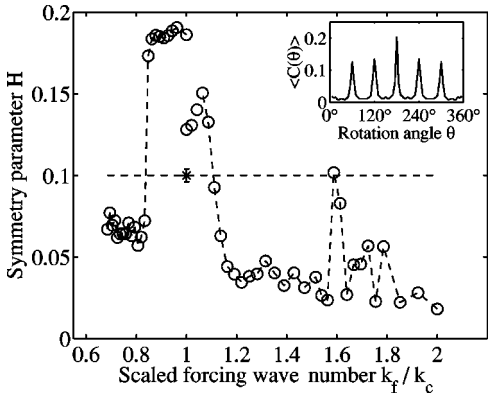

FIG. 5. Change of spatial order: plot of the hexagonal symmetry parameter H, averaged over many snapshots of one sequence, versus scaled forcing wave number. The value for the unforced system (- - ∗ - -) is included for comparison. Strong hexagonal order in the locking regimes corresponds to large values of H. The inset shows a typical average rotational autocorrelation function. Here, peaks at every 60° indicate hexagonal order.

ing pattern. Outside the locking regime, strong dynamics is reflected in a small time constant τ_s, accompanied by low values of the symmetry parameter H. Another, less-pronounced locking regime at about $k_f \approx 1.6 k_c$ can be assigned to an excitation of the second critical wave number at $k_c^{(2)} \approx \sqrt{7/3} k_c$.

The locking appears within a certain range of forcing wave numbers. This is in agreement with the linear stability analysis, predicting that above threshold the critical wave number widens to a whole band. The system can seemingly lock onto any wave number within this band. This also holds for the second, smaller locking regime, belonging to a narrower critical band around $k_c^{(2)}$.

For comparison, the characteristic time constant τ_s and the symmetry parameter H of the unforced system are shown in the plots as well. Forcing outside the locking regimes seemingly does not induce a dynamics with a time constant very different from the unforced system. The motion of defects and domain boundaries and the dynamics of a completely disordered pattern take place on a similar time scale. Only the measure for the spatial order makes clear that the system falls either into a well-ordered or a rather disordered state—both significantly different from the unforced case.

In conclusion, we find that with a weak forcing of the appropriate wave number, it is not only possible to reconstitute the perfect regular hexagonal pattern belonging to the basic critical wave number [6]. We can furthermore excite a pattern of a higher-critical wave number, which is otherwise concealed. So far, we find no indication for an excitation at the second harmonic or locking at other rational multiples of k_c. The locking regimes are in agreement with the linear stability analysis.

Beyond the predictions of the linear theory, we observe that forcing with other than a generic wave number provokes spatiotemporal disorder (''optical turbulence''). This is particularly clear for forcing wave numbers smaller than the critical one, when higher wave numbers are not active. These findings indicate that disorder is provoked by the presence of unfitting spatial scales [15], hinting at competition effects.

Finally, it is also worthwhile to note that—through falling into one of two distinct states—the system performs a very simple, but all-optical image processing task: the discrimination of a particular spatial scale.

The authors would particularly like to thank T. Tschudi for his support, and acknowledge the collaboration with Jenoptik LOS GmbH in Jena. This work was partially financed by the German Federal Ministry of Education and Research (Contract No. 13N7311/8).

[1] N.B. Abraham and W.J. Firth, feature editors, J. Opt. Soc. Am. B **B7**, 948 (1990); *Nonlinear Dynamics and Spatial Complexity in Optical Systems*, edited by R.G. Harrison and J.S. Uppal (SUSSP Publications, Edinburgh, 1992); L.A. Lugiato, editor, Chaos, Solitons and Fractals **4**, 8 (1994); L.A. Lugiato, M. Brambilla, and A. Gatti, Adv. At. Mol. Opt. Phys., **40**, 229 (1998); R. Neubecker and T. Tschudi, editors, Chaos, Solitons and Fractals **10**, 4 (1999).

[2] M.C. Cross and P.C. Hohenberg, Rev. Mod. Phys. **65**, 851 (1993); P. Manneville, *Dissipative Structure and Weak Turbulence* (Academic Press, San Diego, 1990).

[3] R. Martin, A. Scroggie, G.–L. Oppo, and W.J. Firth, Phys. Rev. Lett. **77**, 4007 (1996); S. Juul Jensen, M. Schwab, and C. Denz, *ibid.* **81**, 1614 (1998); E. Benkler, M. Kreuzer, R. Neubecker, and T. Tschudi, *ibid.* **84**, 879 (2000).

[4] E. Benkler, M. Kreuzer, R. Neubecker, and T. Tschudi, J. Opt. A, Pure Appl. Opt. **2**, 303 (2000).

[5] Recently, there had been some debate on the terminology on systems with additionally imposed signals [6,7]. We would suggest the use of the term *control* only when the extra signal is derived from the actual system state, i.e., represents a feedback. In this respect, we here consider *forcing*, which alters the states of the unaffected system.

[6] P.-.Y. Wang, P. Xie, J.–H. Dai, and H.–J. Zhang, Phys. Rev. Lett. **80**, 4669 (1998).

[7] G.K. Harkness *et al.*, Phys. Rev. Lett. **82**, 2406 (1999).

[8] A.H. Nayfeh and D.T. Mook, *Nonlinear Oscillations* (Wiley, New York, 1979).

[9] V. Petrov, Q. Ouyang, and H.L. Swinney, Nature (London) **388**, 655 (1997); A.K. Horvath *et al.*, Phys. Rev. Lett. **83**, 2950 (1999).

[10] M. Lowe, and J.P. Gollub, Phys. Rev. A **31**, 3893 (1985).

[11] G. D'Alessandro and W.J. Firth, Phys. Rev. A **46**, 537 (1992).

[12] S.A. Akhmanov, M.A. Vorontsov, and V.Yu. Ivanov, Pis'ma Zh. Éksp. Teor. Fiz. **47,** 611 (1988) [JETP Lett. **47**, 707 (1988); B. Thüring, R. Neubecker, and T. Tschudi, Opt. Commun. **102**, 111 (1993); F.T. Arecchi, A.V. Larichev, and M.A. Vorontsov, *ibid.* **105**, 297 (1994).

[13] R. Neubecker, G.–L. Oppo, B. Thüring, and T. Tschudi, Phys. Rev. A **52**, 791 (1995); B. Thüring *et al.*, Asian J. Phys. **7(3)**, 453 (1998).

[14] R. Neubecker, B. Thüring, M. Kreuzer, and T. Tschudi, Chaos, Solitons and Fractals **10**, 681 (1999).

[15] G. Schliecker and R. Neubecker, Phys. Rev. E **61**, R997 (2000).

[16] D. Leduc, M. Le Berre, E. Ressayre, and A. Tallet, Phys. Rev. A **53**, 1072 (1995); E.V. Degtiarev and M.A. Vorontsov, J. Mod. Opt. **43**, 93 (1996); M.A. Vorontsov and A.Yu. Karpov, J. Opt. Soc. Am. B **14**, 34 (1997); R. Herrero *et al.*, Phys. Rev. Lett. **82**, 4627 (1999).

[17] R. Neubecker, Opt. Commun. **132**, 593 (1996).